JOURNAL OF SCIENCE TECHNOLOGY AND EDUCATION 8(4), DECEMBER, 2020
ISSN: 2277-0011; Journal homepage: www.atbuftejoste.com

Robust Control of Autonomous Vehicles in the Case of Dangerous Situation

[1]Ahmad Abubakar, [2]Musa Mohammed, [3]Ibrahim Kabiru Dahiru, [2]Sulaiman Haruna Sulaiman, [2]Ibrahim Abdullahi Shehu, [4]Aminu Yahya Zmit
Gipsa Lab University Grenoble, Alpes,
University Grenobles. Alpes France
[2]Department of Electrical Engineering,
Faculty of Engineering,
Ahmadu Bello University, Zaria, Nigeria
[3]Department of Computer Engineering,
Kano State Polytechnic, Kano, Nigeria
[4]Department of Mechanical Engineering,
University Hafr Albaitin, Saudi Arabia.

ABSTRACT
In this work, some full models that are mainly used for the control synthesis have been introduced for vehicles moving at a curve on a rough surface. The safety performance of an autonomous vehicle based on the longitudinal, lateral and yaw dynamics were investigated. Moreover, steering and braking control under dangerous situations and yaw rate dynamics are of interest in this research. The dangerous situation was modelled as an external disturbance to the vehicle, and as such variations were investigated by the implementation of three controllers: LQR, H infinity – one degree and two-degree controllers. After analysis, H-infinity control approached was found to have the best solution for stability control of yaw vehicle dynamics.

ARTICLE INFO
Article History
Received: June, 2020
Received in revised form: July, 2020
Accepted: August, 2020
Published online: November, 2020

KEYWORDS
Autonomous Vehicle, Dangerous Situation, H-infinity control, LQR, Yaw rate.

INTRODUCTION

Advancements in automotive industries have steered towards improving complex system performance and robustness such as vehicles systems through the use of electronic components, microcontrollers and control system technology. In-vehicle technology, Active Safety (AS) and Passive Safety (PS) are always of great interest. The latter is always complementing the former. AS technique focuses on avoiding accidents by facilitating improved vehicle controllability and stability especially when encountering emergency and dangerous situations. Such as what may be experienced when unexpectedly encountering slippery road paths, while PS is concerned mainly with the confidentiality and integrity of the vehicles.

An autonomous vehicular system is a system of the vehicle that is autonomously capable of sensing its environment and moving with little or no human input through the desired trajectory. This area has drawn a lot of research interest from both industries and academia. It is without a doubt that, the technology has broad applications in various disciplines such as construction and mining industries, seaborne shipping vessels, mechanized farming[1] and Unmanned Autonomous Aerial Vehicles (UAVs)[2]. Despite the huge investment in procuring and developing full autonomous vehicle technology, yet it will be decades ahead before commissioning full autonomous vehicle capable of navigating itself through highways and congested cities that require absolute control and fast response. This is due to the safety reason, traffic laws and other related factors. Furthermore, the dynamics of autonomous vehicles are very complex and highly

Corresponding author: Ahmad, A. ahmad.abubakar@gipsa-lab.grenoble-inp.fr Gipsa Lab University Grenoble, University Grenobles. Alpes France Alpes.

nonlinear[3]. However, the vertical action, roll and pitch of the vehicles are generally connected to comfort performances and safety characteristics. Additionally, the safety performance of automotive vehicles is mainly characterized by the lateral, yaw and longitudinal dynamics of the vehicles. These vehicular dynamic features are mostly treated in a decoupled way such that, the longitudinal dynamics are linked to suspension systems while the yaw and lateral dynamics are related to steering and braking systems respectively. A vast number of research works have been carried out on longitudinal vehicle behaviours through the rotational wheel and slip dynamic control, hence leading to the development of Anti-locking Braking System(ABS)[4].

A lot of industrial research and development works are ongoing in the area of design and control of autonomous vehicles[5]. The Tesla Model S driverless is a shared experience of the driving vehicle that uses GPS and sensors in the autopilot mode to ensure the vehicle remains in a steady path on the highway[1]. It alerts the driver when there is proximity to obstacles or other cars and automatically changes lane to prevent an accident. It just requires that the driver hands on the steering wheel at all times. As of 2017 many automobiles such as BMW, Mercedes Benz, Lexus, Volvo and Nissan have these similar features in some of their vehicles designs[1].

Furthermore, there exist many types of research in the control of autonomous vehicles in both industries R&D and academia. This is due to the significant impact that autonomous driving would have on improving road safety and reducing accidents as well as driving associated tedious tasks. However, the research in this area is complex due to the high nonlinearity nature of the system dynamics and strong coupling between the lateral and longitudinal dynamics[6]. Moreover, safe autonomous vehicles require real-time operations and fast responses to the sensor input. The autonomous vehicle driving strategy was classified into two by [7] to include assistant driving and autonomous driving. Assistant driving is the one in which there is shared control of the vehicle and the human driver and involves various strategies such as modelling the driver response into the controller or guiding the driver with little intrusion to the driver except in emergency case or when the driver leaves the safe trajectory. While autonomous driving on the other sides involves complete control of the lateral and longitudinal dynamics of the vehicle. For the control architecture of a fully autonomous vehicle, the authors in [3] describe the various processing stages needed and finally identifies perception, decision and the control as the most important stages.

The authors in [8] have further proposed a coordinated steering and braking control strategy in emergencies and designed an obstacle avoidance for automated driving of vision-based autonomous vehicles. The strong nonlinearity in the system dynamics and high coupling of the longitudinal and lateral dynamics were tackled using the proposed controller on nonlinear back-stepping control theory and adaptive fuzzy sliding-mode control techniques. The reference path detection and real-time location information updates were done using a vision-based algorithm. The proposed coordinated controller was checked for asymptotic convergence using Lyapunov stability theory. The work is concluded with experimental validation on tracking performance and riding comfort.

The work of [9] proposed a shared steering control using steer-by-wire technology with safe envelopes to improve obstacle avoidance and overall vehicle stability. The control problem was formulated as a direct matching of the driver's steering commands with the controller to ensure collision avoidance and vehicle stability. The control strategy used was the model predictive control (MPC) scheme wherein the controller only intervenes when the driver trajectory is not

Corresponding author: Ahmad, A. ahmad.abubakar@gipsa-lab.grenoble-inp.fr *Gipsa Lab University Grenoble, University Grenobles. Alpes France Alpes.*

within the designed safe envelopes. The two envelopes are designed such that one handles the vehicle limit and the other handles the environmental limits such as lane boundaries and obstacles. The strategy is validated on an experimental vehicle in a low friction environment.

Path planning is important for proper control strategy to be developed. Reference [10] presented a review of motion planning techniques for autonomous self-driving vehicles. The authors presented several path planning techniques such as graph search-based planners, the Djiastra algorithm, sampling-based planners, interpolating curve planners, A-star algorithm and state lattices and other numerical optimization approaches.

An ergonomic framework for cooperative guidance and control for autonomous vehicles was presented in [11] with emphasis on the association between the vehicle and humans. Conduct-by-Wire approach in which the said cooperation exist mainly on the guidance level while the driver can manipulate the controller through a specialized manoeuvring interface, and H-Mode techniques which is a haptic-multimodal interaction with highly automated vehicles based on the H-Metaphor in which the cooperation exists mostly on guidance and control with an active interface. These approaches allow for shared control of the vehicle and the controller in such a way that, the driver can actively assign a control action to the controller through the interfaces.

With the review of past works on the different strategy adopted in the control of both fully and semi-automated vehicles and having identified the major areas of operation of an autonomous vehicle as Perception, Decision/Planning and Control, this paper would be focusing on the control strategy of the autonomous vehicle and hence propose a model for the longitudinal and lateral dynamics, and design a robust controller using H-α control for steering and braking control that has minimal intrusion of the driver steering but capable of ensuring the driver is within the desired safe trajectory. Thus, the controller will have the robustness to act in the event of an emergency or dangerous situation.

VEHICLE DYNAMIC MODEL

The full dynamic vehicle model was adopted from the works of Poussot-Vassal *et al* (2011) [3] and Jinghua Guo *et al* (2016)[8]. Accounting for the nonlinear load transfer model, fast dynamics entering in the tyre force description, and the general chassis dynamics are the main reasons behind consideration of the full dynamic model especially in dangerous circumstances. Figure1 presents the model of the vehicle.

It could be seen that models of the longitudinal (xs), lateral (ys), vertical (zs), roll (θ), pitch (ϕ) and yaw (ψ) dynamics of the chassis have all been included in the full dynamic model of the vehicle. The Centre of Gravity (COG) and sideslip angle (β) dynamics as a function of the tyres and suspensions forces were also modelled. The parameters Md, Mdy, Mdz, F, Fdy and Fdz are the rear braking torques input, the roll moment, pitch moment, yaw moment, longitudinal disturbance, lateral disturbance and vertical load disturbance respectively.

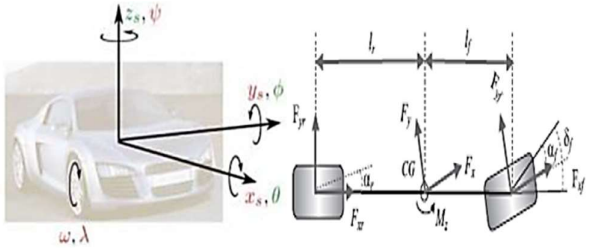

Figure 1: Full Vehicle Model [3, 8]

Corresponding author: Ahmad, A. ahmad.abubakar@gipsa-lab.grenoble-inp.fr *Gipsa Lab University Grenoble, University Grenobles. Alpes France Alpes.*

JOURNAL OF SCIENCE TECHNOLOGY AND EDUCATION 8(4), DECEMBER, 2020
ISSN: 2277-0011; Journal homepage: www.atbuftejoste.com

Let the vehicle parameters be specified as M stand for the total mass of the vehicle, M_r for the rear mass of the vehicle, while I_z, I_x, I_y are the yaw, pitch and roll inertia of the vehicle respectively. C_f defines the front linear tire lateral cornering stiffness, C_r is the rear tires cornering stiffness respectively. Furthermore, let l_r, l_f be the distance of the rear and front axle from the COG and t_r be the rear axle length. Similarly, let R be the radius of the tire, T_{bmax} is maximum braking, '***g***' gravitation acceleration, μ tire to road friction ratio interval and *v* be the vehicle velocity intervals. This full dynamic model of the vehicle was obtained under the following set of assumption [3].

a. Vertical, roll, and pitch motion were ignored
b. Braking and steering dynamics were approximated as linear first-order systems
c. Effects of suspension on the tyre axels were neglected.

The part of the vehicle dynamics that is concerned with the steering and braking control involves the side slip β and the yaw ψ dynamics which can be derived below and presented by equation 6.

By resolving the forces in figure 1, the following equation is obtained.

$$mv1\dot{B} = f_{yf} + f_{yr} + mv\dot{\Omega} \quad (1)$$

$$I_z\ddot{\Omega} = I_f\left(-F_{xf}\,sin(\text{ɤ}) + F_{yf}\,cos(\text{ɤ})\right) - I_r 2F_{yr} - \Delta F_{xr} \quad (2)$$

Where $\beta = \frac{\dot{Y}_s}{\dot{X}_s}$

Similarly; $F_{yf} = F_{yl} + F_{yr}$ and $F_{yr} = F_{yrl} + F_{yrr}$

$$\therefore \Delta F_{xr} = F_{xrl} - F_{xrr}3 \quad (3)$$

The speed in the longitudinal direction can be defined as:

$$v = \sqrt{\dot{x}_s + \dot{y}_s}$$

By expressing equation (3) in terms of braking torque, it can be simplified and presented by equation (4) as;

$$\Delta F_{xr} = F_{xrl} - F_{xrr} = \frac{URmrg}{2}(T_{brl} - T_{brr}) \quad (4)$$

Combining equations (4) and (2) yields equation (5)

$$I_z\ddot{\Omega} = L_f\left(-F_{xf}\,sin(\delta) + F_{yf}\,cos(\delta)\right) - L_rF_{yr} - \frac{URmrg}{2}(T_{brl} - T_{brr})t_r + M_{dz} \quad (5)$$

Linearized model based on the following equilibrium points for ensuring the stability of the system is given by equation 6.

1. Steering angle δ=0
2. Low steering angle cos(δ)=1
3. Low slip angle
4. Low-velocity ratio

•

$$\begin{bmatrix}\dot{\beta}\\ \ddot{\Omega}\end{bmatrix} = \begin{bmatrix}\mu - \frac{C_f - C_r}{mv} & 1 + \mu\frac{l_rC_r - l_fC_f}{mv}\\ \mu\frac{l_rC_r - l_fC_f}{I_z} & \mu\frac{-l_f^2C_f - l_r^2C_r}{I_zv}\end{bmatrix}\begin{bmatrix}\beta\\ \dot{\Omega}\end{bmatrix} + \begin{bmatrix}\frac{C_f}{mv} & 0 & 0\\ \frac{I_fC_f}{I_z} & \frac{-\mu m_r g R t_r}{2I_z} & \frac{\mu m_r g R t_r}{2I_z}\end{bmatrix}\begin{bmatrix}\delta\\ Tb_{rl}\\ Tb_{rr}\end{bmatrix} + \begin{bmatrix}0\\ \frac{1}{I_z}\end{bmatrix}M_{dz} \quad (6)$$

CONTROL DESIGN

A. This section discusses the problem formulation, control objectives and the general control structure. The overall control structure is shown in figure 2 and 3, while the main control objectives are as follows:

(1) Improve driving comfort performances by minimizing the yaw rate error concerning a reference provided by the reference model.

(2) Ensuring that the braking control signal is always achieved through the steering control actuators.

(3) Improving the general system performance under critical situations or actuator failure.

Corresponding author: Ahmad, A. ahmad.abubakar@gipsa-lab.grenoble-inp.fr Gipsa Lab University Grenoble, University Grenobles. Alpes France Alpes.

JOURNAL OF SCIENCE TECHNOLOGY AND EDUCATION 8(4), DECEMBER, 2020
ISSN: 2277-0011; Journal homepage: www.atbuftejoste.com

Based on the control problem formulation defined in Figure 2, a generalized control scheme for H-infinity control problem which comprises the plant and the controllers is illustrated in figure 3.

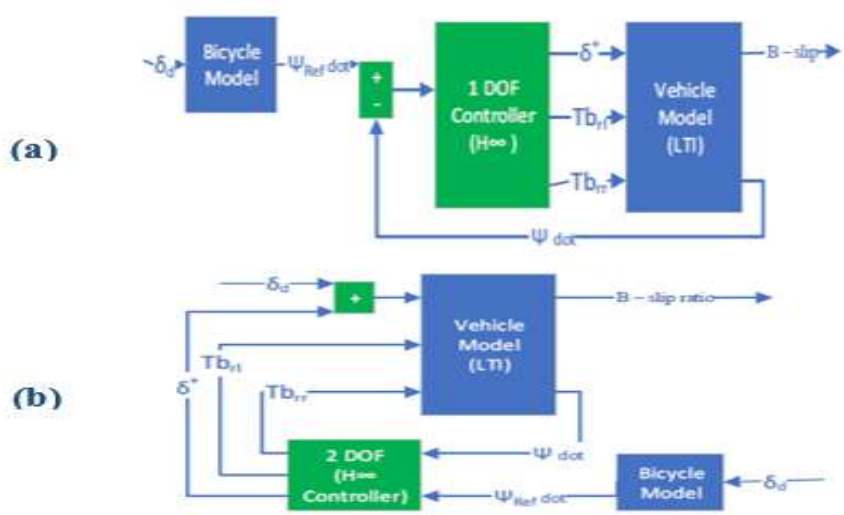

Figure 2: (a) One Degree Control Structure, (b) Two-Degree Control Structure

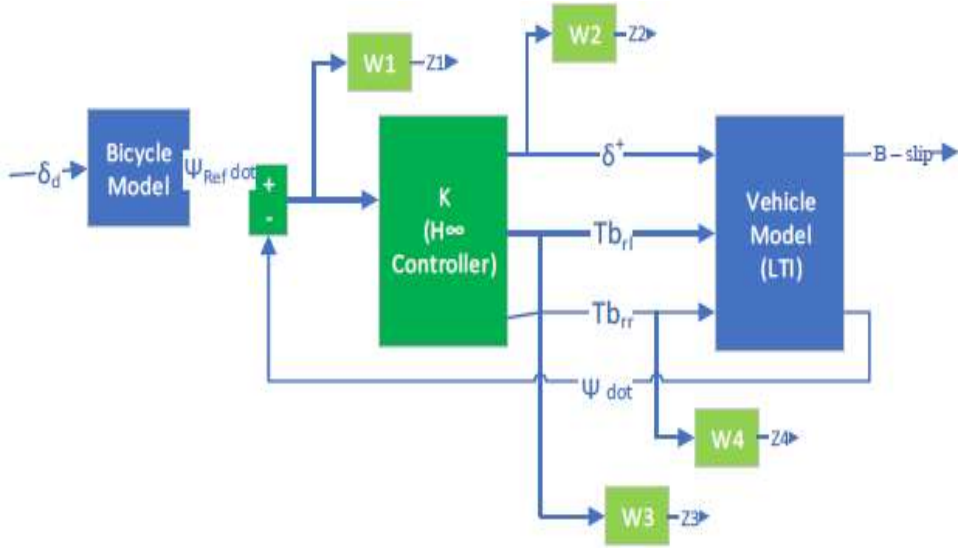

Figure 2: H-infinity Control Scheme

In defining the performance specifications, the approach of Poussot-Vassal *et al* in [7] was adopted. The weighting functions are used to describe the performance objectives and steering actuator frequencies limitations as follows:

- **Z_1** is the output tracking error performance weight define by the yaw rate error exogenous output signal as in (7).

$$W_1 = 12\gamma\left(\frac{\frac{S\gamma}{2\pi f_1}+1}{S/_{2\pi f_1}+1}\right) \qquad (7)$$

Corresponding author: Ahmad, A. ahmad.abubakar@gipsa-lab.grenoble-inp.fr *Gipsa Lab University Grenoble, University Grenobles. Alpes France Alpes.*

JOURNAL OF SCIENCE TECHNOLOGY AND EDUCATION 8(4), DECEMBER, 2020
ISSN: 2277-0011; Journal homepage: www.atbuftejoste.com

Where $f1$ = 1Hz define as the cut-off frequency of the high-pass filter, γ= 0.1 the attenuation level for low-frequency yields (static tracking error ≤ 10%).

- **Z_2** define as the exogenous steering control signal attenuation, defined by the output steering control performance weight as:

$$W_2 = G_\propto \left(\frac{\left(S/_{2\pi f_2+1}\right)}{\left(S/_{\delta 2 f_3+1}\right)^2} \right) \quad (8)$$

Where $f3$ = 10 Hz define the bandwidth of the steering actuator and $f2$ = 1Hz define as the lower limit frequency of the steering actuator. Hence the frequencies f2 and f3 are the filter frequencies bands designed to confine the steering system to operate within the region of interest [$f2$, $f3$]. While the steering action is allowed, the gain amplification is bounded by$G\delta = 5 \times 10^{-3}$. Thus, the inclusion of such filter is to allow the steering system act at those frequencies bands which the driver is unable to provide. They also handle steering actuator drawbacks.

Z_3 = Z4, are the exogenous braking control signal attenuation which is defined by the braking control weights outputs as:

$$W_3 = W_4 = G_T \left(\frac{S/_{2\pi f_4+1}}{S/_{\alpha 2\pi f_4+1}} \right) \quad (9)$$

Where $f4$ = 10 Hz is the bandwidth of the braking actuator, α=100 is the roll-off parameters (must be selected such as to handle the dynamical braking actuator limitations) and $G = 4 \times 10^{-4}$ selected to have a very good amplification gain of the control input to avoid saturation of control signal. Now, to obtain the generalized model of the plant P for the mixed sensitivity H-infinity control problem as shown in figure 4, the following variables can be defined as follows:

$w(t) = [\psi_{ref}(t), Mdz(t)]$ = The exogenous input signals
$u(t) = [\delta^*(t), T^*brl(t), T^*brr(t)]$ = Control Input signal
$y(t) = [e\psi(t)]$ = Signal measurement output
$z(t) = [Z_1(t), Z_2(t), Z_3(t)]$ = Output control signal

$$P: \begin{cases} \dot{x}(t) = Ax(t) + B_1 w(t) + B_2 u(t) \\ Z(t) = C_1 x(t) + D_{11} w(t) + D_{21} u(t) \\ y(t) = C_2 x(t) + D_{21} w(t) \end{cases} \quad (10)$$

Now, the control objective is to obtain a state feedback control law:
$U(t) = -kx(t)$ Such that
$\|T_{zw}(s)\|_\alpha = \gamma$
Complete Simulink block for both one degree and two-degree H-infinity controllers is presented by figure 5.

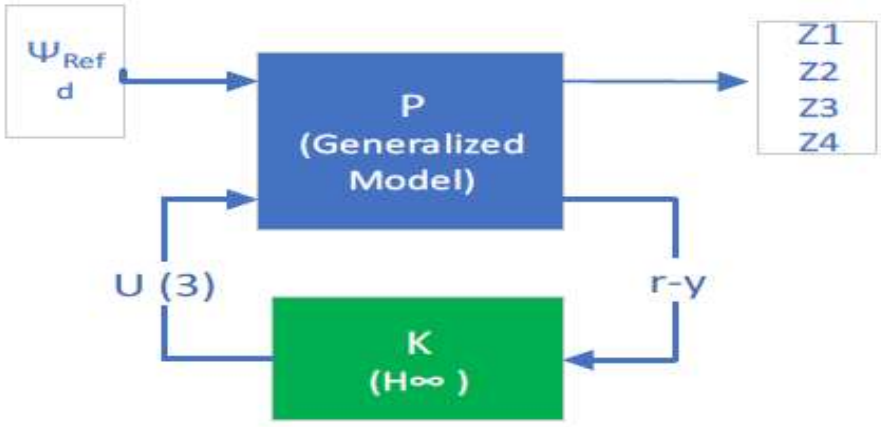

Figure 3: Generalized plant

Corresponding author: Ahmad, A. ahmad.abubakar@gipsa-lab.grenoble-inp.fr Gipsa Lab University Grenoble, University Grenobles. Alpes France Alpes.

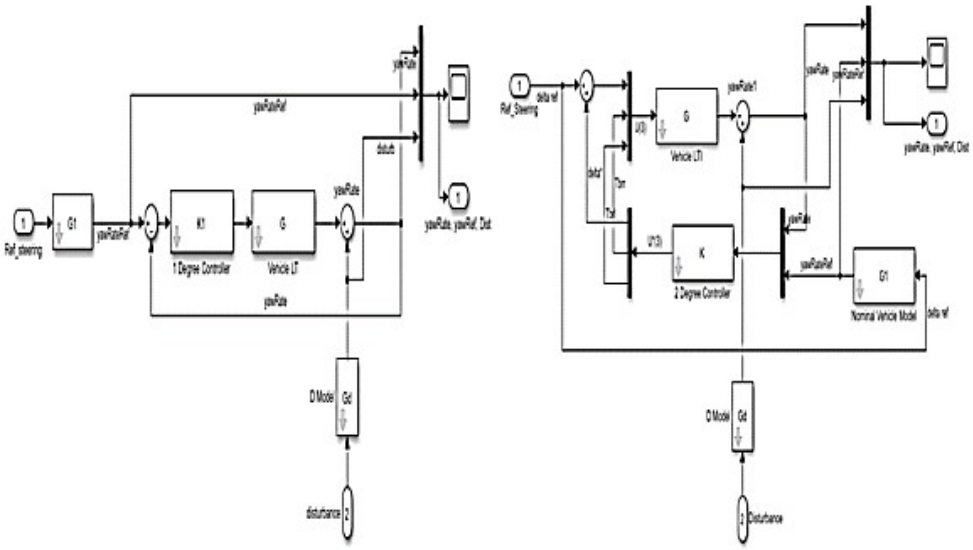

Figure 4: One Degree and Two Degree of Freedom H_{inf} Controllers Simulink Blocks

LQR Controller Design

The design of an LQR controller aims at optimizing an energy function, 'J' by obtaining optimal state feedback controller gain 'K'. The LQR control block diagram representation is as shown in figure 6.

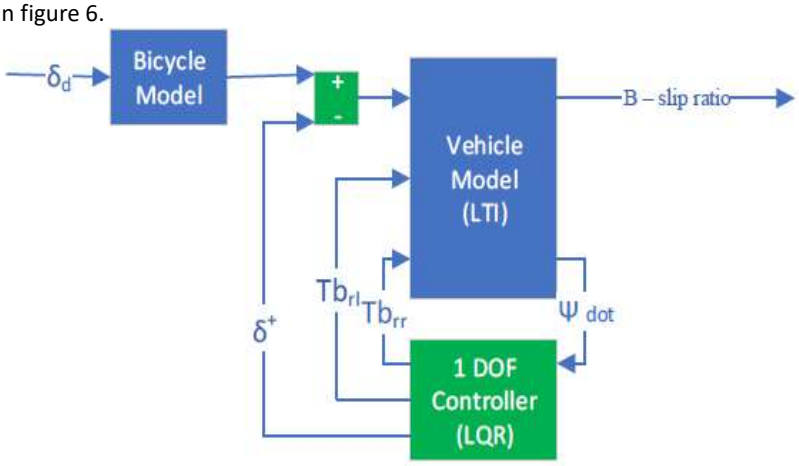

Figure 5: LQR Control Block

A general state variable form is defined by (11)

$$G: \begin{cases} \dot{x}(t) = Ax(t) + Bu(t) \\ y(t) = Cx(t) \end{cases} \quad (11)$$

Where *x, u* represents the system states and the control input. The initial condition is assumed to be 0 and the states x (t) are measurable. Equation (12) gives the state-variable feedback control law.

$$u(t) = -kx(t) \quad (12)$$

Where k is the feedback control gain. Similarly, the closed-loop system using this control law can be obtained as in equation (13)

$$\dot{x} = (A - Bk) \quad (13)$$

A good LQR controller design is expected to find the optimal control law

Corresponding author: Ahmad, A. ahmad.abubakar@gipsa-lab.grenoble-inp.fr *Gipsa Lab University Grenoble, University Grenobles. Alpes France Alpes.*

JOURNAL OF SCIENCE TECHNOLOGY AND EDUCATION 8(4), DECEMBER, 2020
ISSN: 2277-0011; Journal homepage: www.atbuftejoste.com

that minimizes the following performance index:

$$J = \int [x^t(t)Qx(t) + u^T(t)Ru(t)]dx \quad (14)$$

Where *J* is the energy function, Q is a symmetric semi-positive definite matrix and R is a positive scalar. u(t) is the optimal input follows from the first necessary condition of optimality that:

$$u(t) = -R^{-1}B^T Px(t) \quad (15)$$

In order to find P, the algebraic Ricatti equation is used which is define as:

$$PBR^{-1}B^T P + Q = 0 \quad (16)$$

Thus, the control gain can be defined as K:

$$K = R^{-1}B^T P$$

The Simulink control block for LQR is given by figure 7

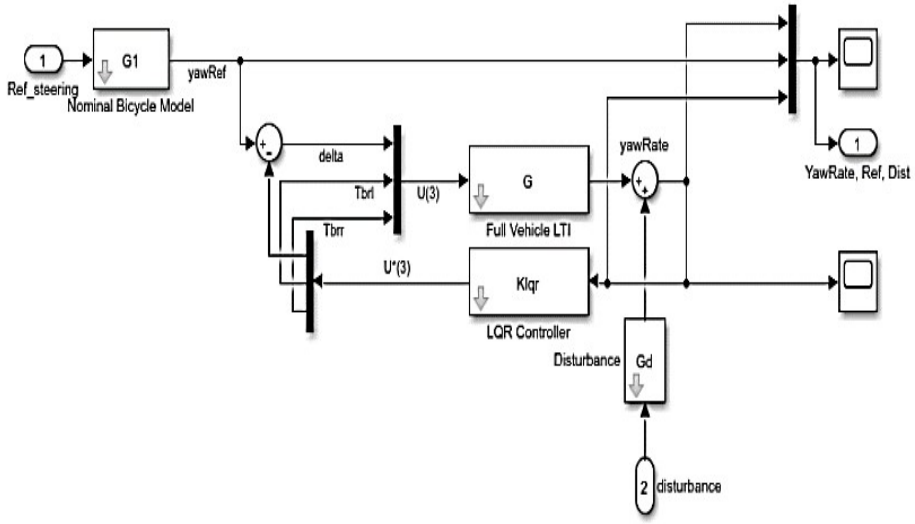

Figure 6: LQR Control Simulink Block

RESULT AND DISCUSSION

Stability Analysis

Stability analysis is carried out on the system model to ascertain the controllability and observability state of the system before designing the intended control algorithm (H $_{\text{infinity}}$ and LQR). By substituting the values of the parameters and variables in equation (6); to obtain the Eigen values of the model as shown in figure 8 below.

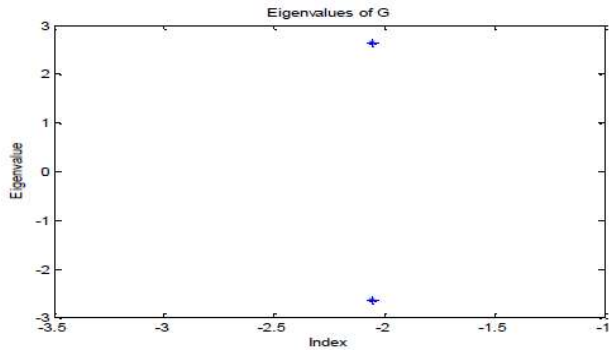

Figure 7: Eigen Value poles plot test for stability

Corresponding author: Ahmad, A. ahmad.abubakar@gipsa-lab.grenoble-inp.fr Gipsa Lab University Grenoble, University Grenobles. Alpes France Alpes.

JOURNAL OF SCIENCE TECHNOLOGY AND EDUCATION 8(4), DECEMBER, 2020
ISSN: 2277-0011; Journal homepage: www.atbuftejoste.com

Additionally, Kalman's test describes by equations (17) and (18) were used to test for the system model's controllability and observability respectively.

$$K_T = \begin{cases} M_C = [B\ AB\ A_2B] \\ M_O = [C_T\ \ A_TC_T\ A_{T2}T_T\ ] \end{cases} \quad (17)$$

Where M_c and M_o are the controllability and observability matrices respectively. The following observation was made from the two tests:

OBSERVATION:

I. From figure 8, all the Eigen values have a negative real part that is Re (λ) ≤ 0.

II. From Kalman's stability test, the ranks of [M_C] and [M_O] ≠ 0 and rank of K_T = 2.

This is the same as the number of states of the system. Thus, from the above two tests, the system generally states controllable as well as observable.

Performance Analysis using Frequency response (Sensitivity functions)

Consider the following frequency responses shown in figures 9-14 as obtained from H-infinity control and LQR control approach. Detail analysis and performance evaluation can be described as follows.

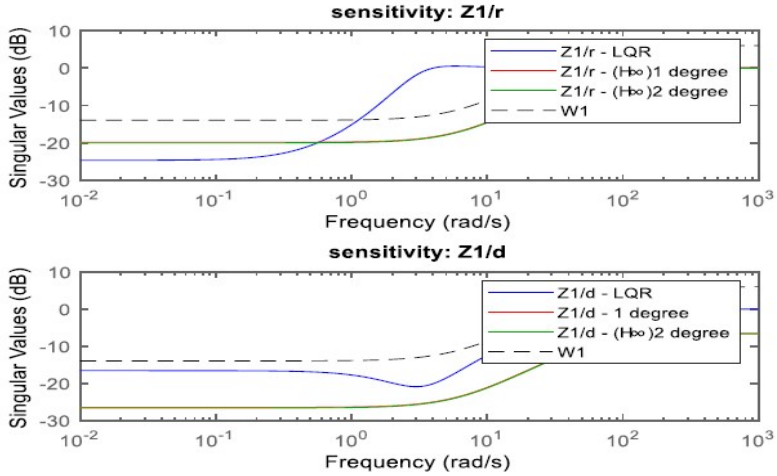

Figure 8: Yaw rate Sensitivity function Sr(jw) and Sd(jw)

Analysis of the Sensitivity function

Figure 9 shows the sensitivity function performance analysis of the 1 degree, 2-degree H-infinity and LQR controllers. The defined performance specification is given by W1. The results show that the 1 degree and 2 degrees H-infinity controllers have improved tracking performance compared to LQR. This is because the peak value of the LQR controller and the overshoots is beyond the control performance specifications. Furthermore, the result shows that the LQR has a less steady-state error in tracking than the H- infinity controllers. Moreover, in disturbance rejection at low frequency, the H infinity controllers have better disturbance rejection, unlike the LQR controller.

Analysis of the Steering control Sensitivity function

Figure 10 gives steering control sensitivity function. The steering control output for all the controllers is consistent with the designed specification. Although, the 2-degree controller has the better roll-off at high frequency and thus has better noise attenuation than the 1-degree and

Corresponding author: Ahmad, A. ahmad.abubakar@gipsa-lab.grenoble-inp.fr Gipsa Lab University Grenoble, University Grenobles. Alpes France Alpes.

LQR controllers. For the H∞ controllers, they act well within the specified frequency ranges (f2 – f3) and as such preserve the bandwidth of the steering system. Unlike the LQR whose roll off and bandwidth is not as good as the H infinity controllers.

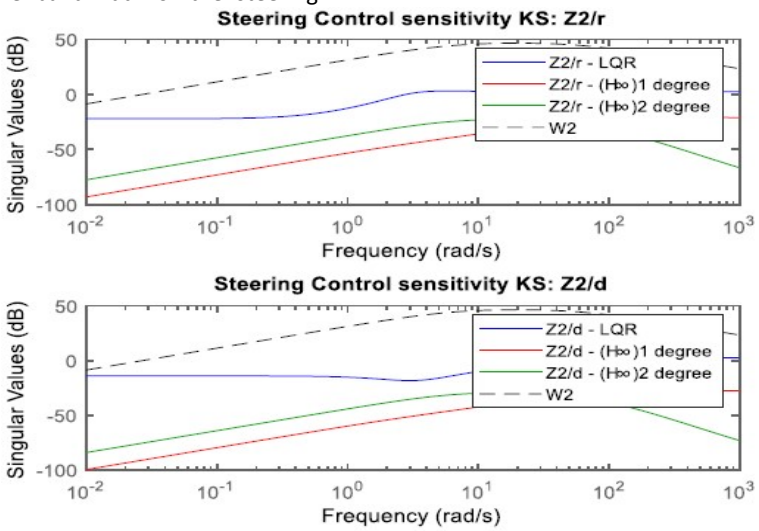

Figure 9: Steering Control sensitivity function KSdr and KSdd

Analysis of the Braking control Sensitivity function

Figure 11 shows the braking control sensitivity functions. The left and right braking torques have the same sensitivity functions. The braking rolls off after frequency above the specification frequency f4 = 10Hz. This ensures that the braking control has good attenuation to measurement noise at high frequency. In terms of input saturation, the 2-degree H infinity controller has a higher tolerance for the input. In summary, the 2-degree controller has a better overall performance.

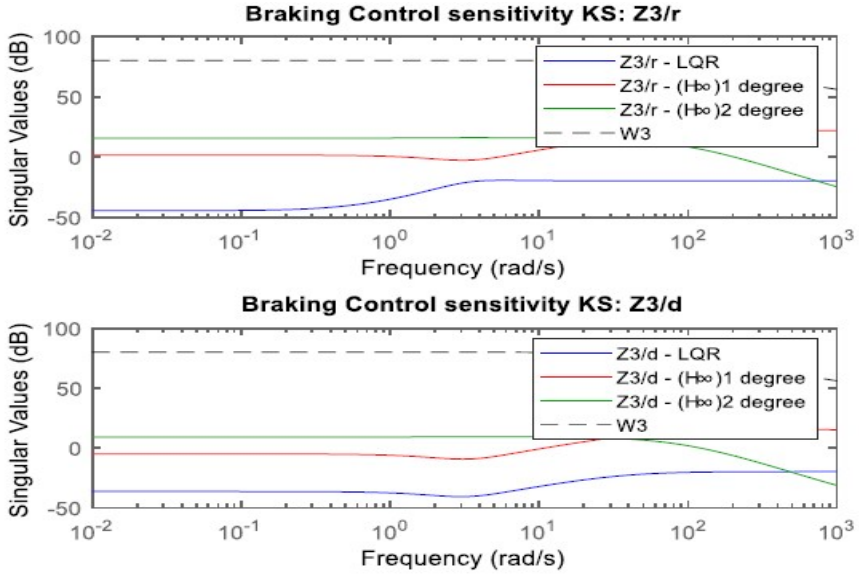

Figure 10: Braking Control sensitivity function KSbr and KSbd

Corresponding author: Ahmad, A. ahmad.abubakar@gipsa-lab.grenoble-inp.fr Gipsa Lab University Grenoble, University Grenobles. Alpes France Alpes.

Performance Analysis using Time response

In defining the steering angle signal as the reference, the approach in reference [3] was adopted. Furthermore, MATLAB code is designed and generates the steering reference signal as shown in figure 12.

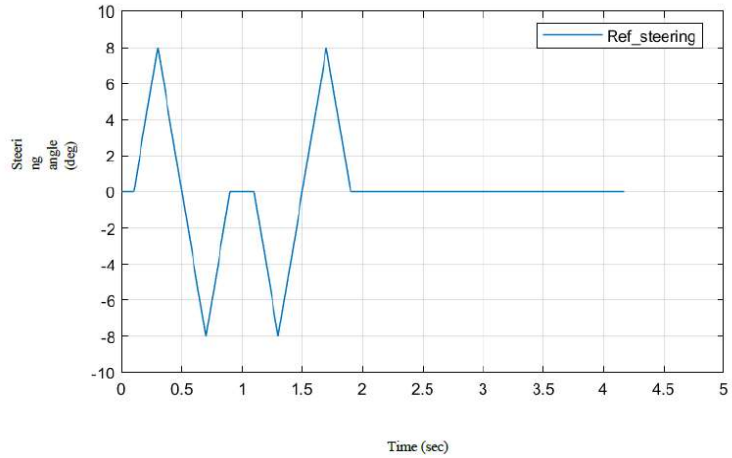

Figure 11: Generated Steering angle signal

After running the implemented control in figure 8 and 10, the result is obtained as shown in figure 13 below, with Redline: Reference yaw rate, Blue line: one-degree H-infinity controlled output Purple line: two-degree H-infinity controlled output, Pink line: LQR controlled output, Orange line: Disturbance effect.

Thus, from the summary table, although all the controllers enhance yaw rate tracking and robustness concerning uncertainties (vehicle or road disturbance) but still we can conclude that H-infinity control approached has the greatest tracking performance improvement and more robust to uncertainty compare to LQR control approach.

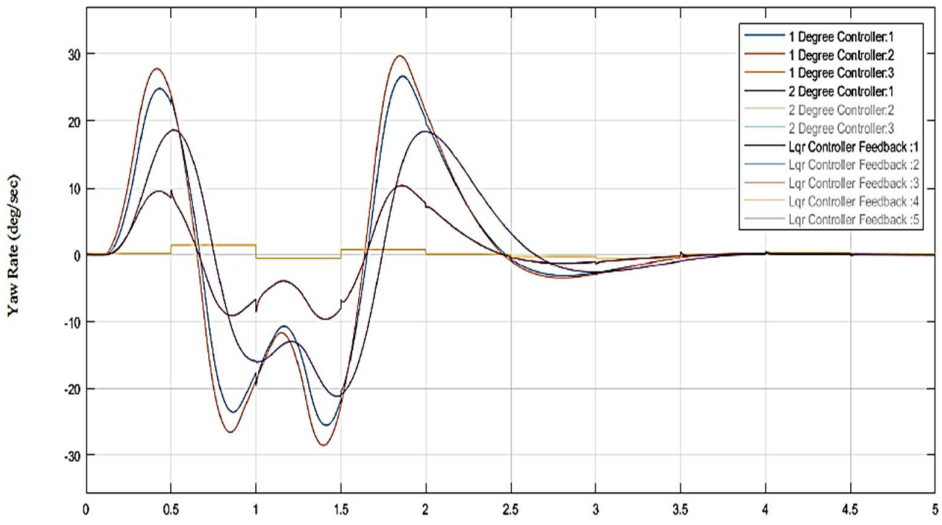

Figure 12: Time response for the control system

Corresponding author: Ahmad, A. ahmad.abubakar@gipsa-lab.grenoble-inp.fr Gipsa Lab University Grenoble, University Grenobles. Alpes France Alpes.

Table 1: Comparison between the H-infinity controlled response and LQR control response

Controller	Tracking performance	Settling time(sec)	Reduction in Yaw rate error (%)	Robustness to uncertainty
One degree H-infinity control	Best	2.1	10	Better
Two degree H-infinity control	Better	3.2	35	Best
LQR control	Good	4.0	65	Good

CONCLUSION

In this article, some full vehicle models have been introduced while moving at a curve on a rough surface. These models are mainly used for control synthesis. The interest is in investigating the safety performance of an autonomous vehicle based on the longitudinal, lateral and yaw dynamics. Moreover, in our area of interest for steering and braking control under the dangerous situation, the dynamics of interest is the yaw rate dynamics and as such the output of our model is the yaw rate. The dangerous situation is modelled as an external disturbance to the vehicle, and as such variations are investigated by the implementation of three controllers: LQR, H-infinity one degree and two-degree controllers. After analysis, H-infinity control approached has the best solution for stability control of yaw vehicle dynamics.

REFERENCES

1. Jones, L., Driverless cars: when and where? Engineering & Technology, 2017. 12(2): p. 36-40.
2. Nadir, B.M., Z. Zhibin, and M. Benbouzid, A critical review on unmanned aerial vehicles power supply and energy management: Solutions, strategies, and prospects. Applied Energy, 2019. 255: p. 113823.
3. Poussot-Vassal, C., O. Sename, L. Dugard and S. M. Savaresi Vehicle dynamic stability improvements through gain-scheduled steering and braking control. . Vehicle System Dynamics, (2011). 49:10, : p. 1597–1621.
4. Chen, J. and G. Tan. Study of Anti-lock Brake System Control Strategy in Automobile. in International Conference on Computer Science, Environment, Ecoinformatics, and Education. 2011. Springer.
5. Duarte, F. and C. Ratti, The impact of autonomous vehicles on cities: A review. Journal of Urban Technology, 2018. 25(4): p. 3-18.
6. Chebly, A., R. Talj, and A. Charara, Coupled longitudinal and lateral control for an autonomous vehicle dynamics modelled using a robotics formalism. IFAC-PapersOnLine, 2017. 50(1): p. 12526-12532.
7. You, C., et al., Advanced planning for autonomous vehicles using reinforcement learning and deep inverse reinforcement learning. Robotics and Autonomous Systems, 2019. 114: p. 1-18.
8. Jinghua Guo, P.H., and Rongben Wang ''Nonlinear Coordinated Steering and Braking Control of

Corresponding author: Ahmad, A. ahmad.abubakar@gipsa-lab.grenoble-inp.fr Gipsa Lab University Grenoble, University Grenobles. Alpes France Alpes.

Vision-Based Autonomous Vehicles in Emergency Obstacle Avoidance'',. IEEE Transactions on Intelligent Transportation Systems, 2016. 17(1,).

9. Stephen M., S.F., & Joseph Christian G., ''Shared Steering Control Using Safe Envelopes for Obstacle Avoidance and Vehicle Stability''. , IEEE Transactions on Intelligent Transportation Systems, (2016). , Vol. 17, No. 2.

10. David G., J.P., Vicente M., and Fawzi N., ''A Review of Motion Planning Techniques for Automated Vehicles''. IEEE Transactions on Intelligent Transportation Systems, 17(4), (2016).

11. Frank O., K.B., Heiner B., Hermann W.& Ralph B., ''Towards cooperative guidance and control of highly automated vehicles: H-Mode and Conduct-by-Wire'', Ergonomics, 57(3): p. 343-360.

Corresponding author: Ahmad, A. ahmad.abubakar@gipsa-lab.grenoble-inp.fr Gipsa Lab University Grenoble, University Grenobles. Alpes France Alpes.